Adaptive time stepping approach forPhase-Field modeling of phase separation and precipitates coarsening in additive manufacturing alloys- COMPLAS 2021

Seifallah Fetni*, Jocelyn Delahaye †, Lauren Duchêne *, Anne Mertens †, Anne Marie Habraken *

* University of Liège, UEE Research Unit, MSM division, allée de la Découverte, 9 B52/3, B 4000 Liège, Belgium
E-mail: s.fetni@uliege.be

† University of Liège, Aerospace & Mechanics, MMS Unit, allée de la Découverte, 9 B52/3, B 4000 Liège, Belgium

ABSTRACT

In the present work, the capacity of phase field method to highlight microstructural changes during the spinodal decomposition of a given binary alloy basing on the Cahn-Hilliard equation is presented. Then, growth and coarsening of precipitates are studied using the KKS (Kim-Kim-Suzuki) model, which includes Cahn-Hilliard and Allen-Cahn equations. The implementation of time stepping algorithms to resolve Phase-Field equations is illustrated. Within Fourier space, using semi-implicit spectral method, it has been demonstrated that it allows faster computing than schemes based on finite difference method. First, spinodal decomposition of a given binary alloy under isothermal loading is implemented and three time stepping approaches are applied: constant time stepping, non- iterative and an iterative method. While the non-iterative method is faster than the constant time stepping scheme, the iterative one, althoughrelatively more CPU consuming,can guaranteethe convergence of the computing. These methods are combined in an innovative approach tested on 1D, 2D and 3D grids. The effectiveness of the adopted adaptive time-stepping algorithm allows resolving equations in reasonable CPU time. It predicts different physical phenomena,such as phase separation and growth and coarsening of precipitates induced by important interfacial energies.

Key words: Phase-Field method, AlSi10Mg, adaptive time stepping, Cahn-Hilliard, Allen-Cahn, Semi-implicit spectral method

1 INTRODUCTION

During a Selective Laser Melting (SLM) process, also named Laser Powder Bed Fusion (LPBF), applied thermal cycles and solidification velocities are considerably increased when compared to ordinary directional solidification. That results in a very fine cellular-dendritic, out-of-equilibrium and inhomogeneous microstructure. Indeed, during the SLM process, various phenomena occur such as heat transfer, fluid flow, moving boundaries and crystalline anisotropy [1].

AlSi10Mg alloy, additively manufactured, is widely used in automotive and aerospace. The prediction of its long-term behavior is of interest and strongly linked to its original state after solidification and heat treatment. Standard analytical methods are not enough to assess the mechanical and thermo-physical properties of the formed microstructure. In several simulations of SLM processes, thermo-physical data are either taken constant in the most simplified models or, if based on measurements, related to material samples generated by another process, while real properties are indeed different [2]. Therefore, the correct thermo-physical properties of the material in its current state should be taken into account during manufacturing or post-treatments.

The number of numerical models of microstructural evolution in materials science has been increased in recent years. Microstructure evolution in Additive Manufacturing (AM) has been intensively investigated by means of cellular automaton, finite element, and phase-field methods. Cellular automaton method has been applied, as a mesoscale approach, to predict grain growth during solidification and give insights about their distributions [3]. Nevertheless, in some case, this method is not efficient for modeling the evolution of the most influential parameters on mechanical properties. It is the case of the alloying concentrations in aluminum alloys (Si in AlSi10Mg or Sr in Al–Sr alloys). Even if phase field method (PFM) is relatively a new approach, it has become more and more recommended for prediction of the formed microstructure under the different driving forces such as thermal gradients, stress and magnetic fields [3, 4]. However, it should be highlighted that one of the limits for the use of this approach is the physical interface width, which is of the order of few nanometers. In order to conduct simulations at larger length scales and decouple interfacial energy from the thickness of the interface, the Kim-Kim-Suzuki (KKS) model [5] has been introduced and its applications in microstructural simulations have been significantly increased [6]. In such a model, different contributions are present: the chemical free energy, double well-potential, phase field gradient as well as the elastic misfit strain energy between the precipitates and the matrix during precipitates growth and coarsening.

In order to ensure the balance between accuracy of calculation and CPU time when taking into account the different contributions, adaptive time stepping was proposed [7, 8]. By literature, different approaches of time stepping were applied to resolve PF equation, such as Cahn-Hilliard (CH) for conservative order parameters [8, 9], Allen-Cahn (AC) for non-conserved order parameters [9] and Phase-Field Crystal (PFC) model [7, 10]. The proposed adaptive stepping methods could be classified following two criteria: the numerical scheme on a one hand and the methodology of adaptive time stepping on the other hand. Numerical schemes should ensure unconditionally energy stability during computing. One can enumerate: backward Euler scheme based on semi-implicit discretization in time [10], linear splitting schemes [11] and Fourier spectral method [12, 13]. For the methodologies of time stepping, they can be, by themselves, classified in iterative [9, 14] and non-iterative ones [8, 15].

The aim of this work is to accurately consider the different energies influencing the final microstructure of the AlSi10Mg during heat loading. It is important to choose the methodology of the numerical implementation of the KKS model in order to ensure the good convergence of the solution with a reasonable CPU time.

This work is divided in two main parts. In the first one, we explore the performance of the Fourier spectral method by implementing a semi-implicit scheme and comparing it to a classical Finite Difference (FD) one. Three methodologies of time-stepping are applied and compared. Numerical implementation targets the CH equation for spinodal decomposition (isothermal loading) of a given binary alloy. Once the first goal (concentration prediction) is achieved and the innovative time-stepping strategy is described, the second part of the article presents the application of this method on the KKS model (considering both CH and AC equations), to study the growth and coarsening of Si precipitates in AlSi10Mg, which is here approximated as a binary alloy.

2 Numerical method

2.1 Governed equations and free energy expressions

2.1.1 Spinodal decomposition

The spinodal decomposition of a binary alloy (Al-Si for example) is governed by the

CHequation expressed as:

$$\frac{\partial X}{\partial t} = \nabla M.\nabla \left(\frac{\delta G}{\delta X}\right) \quad (1)$$

Where*G* denotes the total free energy of the binary alloy, *M* the mobility and *X* the concentration (molar fraction) of one element (Si in AlSi10Mg for example).

When neglecting the terms related to the elastic strain, *G*can be expressed as:

$$G(X) = \int_V [\ g(X) + \frac{1}{2}\kappa(\nabla X)^2]\ dV \quad (2)$$

$\kappa$is here the gradient energy coefficient and g is the chemical bulk energy ; it can be expressed as a 4^{th} polynomial in function of *X*: $g(X) = AX^2(1-X^2)$, *A* is a constant.
Equation 1 could be written as follows:

$$\frac{\partial X}{\partial t} = \nabla (M.G_{XX} \nabla X) \quad (3)$$

$$\frac{\partial X}{\partial t} = \nabla (M).\nabla \left(\frac{\delta g}{\delta X} - \kappa \nabla^2 X\right) \quad (4)$$

Where$G_{XX}$the second derivative of *G* with respect to *X*. Equation 4 is offers an easy implementation of the semi-implicit scheme in Fourier space as follows:

$$\frac{\{X\}_k^{n+1} - \{X\}_k^{n+1}}{\triangle t} = -k^2 M\{\frac{\delta f}{\delta X}\}_k^n - k^4 M\kappa\{X\}_k^{n+1} \quad (5)$$

Here $\triangle t$ is the time step,k is the frequency vector of dimension in Fourier space and n is the time step. $\{.\}_k^n$is the fast Fourier transform (fft) of the given function at the time t^n. $\{X\}_k^{n+1}$ is expressed as a function of $\{X\}_k^n$in a semi-implicit scheme:

$$\{X(k,t)\}_k^{n+1} = \frac{\{X(k,t)\}_k^{n+1} - k^2 M\kappa\{\frac{\delta f}{\delta c}\}_k^n}{1+k^4 M\{c\}_k^{n+1}} \quad (6)$$

2.1.2 Coarsening of precipitates

The KKS model is based on CH equation (eq. 1) for the conservative PF on a one hand and AC equation for the non-conservative PF on the other hand as follows:

$$\frac{\partial \eta}{\partial t} = -L\ \frac{\delta G}{\delta \eta} \quad (7)$$

Here *L* is the kinetic interface coefficient andη is the order parameter (non-conservative PF). The higher is *L*, the more diffusive is the interface. At each time step, η takes 1 as value in the Si precipitate and 0 in the Al matrix.

As illustrated in [16], the total free energy in the KKS model is composed of three kinds of energies as follows:

$$G = \int_V [f_{chem}(X,\eta,t) + \frac{\kappa^2}{2}(\nabla \eta)^2\ + f_{el}(\eta)]\ dV \quad (8)$$

Here f_{chem} is the chemical free energy (also called molar free energy because it depends on the concentration),$\frac{\kappa^2}{2}(\nabla \eta)^2$ is the interface contribution, while f_{el} is the elastic energy due to precipitates misfit.

2.2 Time stepping strategy

For the simulation of spinodal decomposition using CH equation, it should be noted that equation 1 could also be written:

$$\frac{\partial X}{\partial t} = \nabla M.\nabla(\mu) \quad (9)$$

Where$\mu = \frac{\delta G}{\delta \eta}$ is the chemical potential. It could be inferred from the expression above that the energy trends to decrease with time due to gradient-type dynamical equation. Zhang et al. [7] proposed a method for time stepping based on the time derivative (*G'*) of the total free energy:

$$\triangle t = max(\triangle t_{min}, \frac{\triangle t_{max}}{\sqrt{1+\alpha\ G'(t)^2}}) \quad (10)$$

α is a constant to adjust by experience in order to control the level of adaptivity. This method is not iterative and allows a simple adaptivity of the time step $\triangle t$ depending on the energy derivative level. Within the iterative methods, the one proposed by [9] is very interesting as it is based on a norm criterion. The residual value of the computed free energy defines the next time step:

For each time step:

- Step 1: compute X^{n+1} and obtain:

$$RE^{n+1} = \frac{\epsilon(\phi^{n+1})-\epsilon(\phi^n)}{\triangle t^n} + \int_V |\nabla \mu^{n+\frac{1}{2}}|^2 dV \quad (11)$$

here $t^{n+\frac{1}{2}} = (t^n + t^{n+1})/2$ and ϕ is the considered PF ($\eta\ in\ our\ case$).

- Step 2: if $RE^{n+1} > resmax$ take $\triangle t^{n+1} = \triangle t^n/\theta$ and go to step 1
- Step 3: if $RE^{n+1} < resmin$ take $\triangle t^{n+1} = \theta \triangle t^n$

The limits resmax and resmin as well as the parameter θ are obtained by trial and error.

Within the methods ensuringadaptivity [8, 14, 17], we selected the methods [7, 9] because of following advantages: energy dependency, number of unknown to adjust as well as fitting and easy implementation on the semi-implicit spectral scheme. In the next section, we call Method 1 the one of Zhang et al. [7] and Method 2 the one of Guillén-González et al. [9].

3 Results and discussion

3.1 Spinodal decomposition

For the simulation of spinodal decomposition using CH equation with semi-implicit spectral method, 1D, 2D and 3D grids were selected: (N_x=128) for 1D, (N_x=N_y=128) for 2D and (N_x=N_y=N_z=64) for 3D. The grid spacing was set: dx=dy=dz=1nm. It has been then converted to dimensionless grid for computing. A constant mobility (*M*=1) is chosen. The coefficients *A* and κ are respectively set to 1 and 0.5. Results of spinodal decomposition of the binary alloy is shown in Figure 1. Starting from a uniform concentration, isothermal spinodal decomposition tends to reach a periodic concentration pattern.

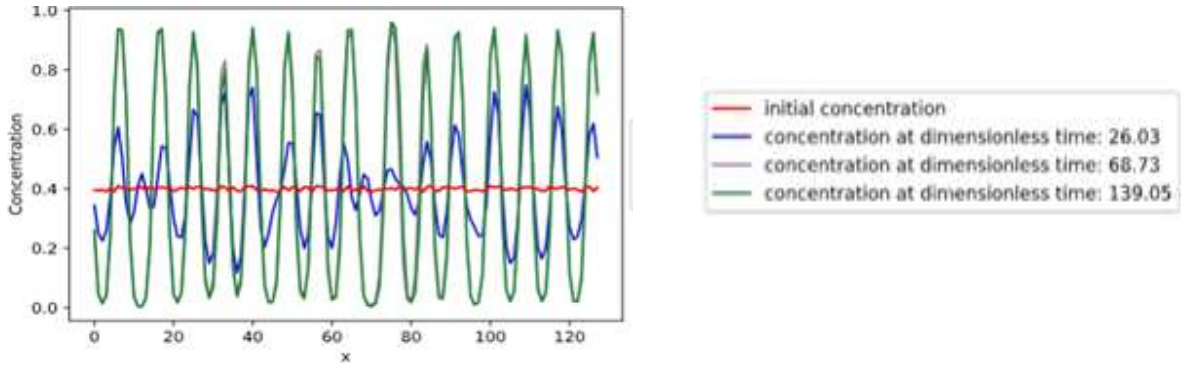

Figure 1: Spinodal decomposition of binary alloy (1D simulation).

Before testing the methods 1 and 2 on Equation 1, a set of 2D simulations, using a constant time step approach, was conducted. The aim of this trial is to see the influence of the time-stepping on the energy evolution during decomposition. As shown in Figure 2, it can be easily inferred that the range of time steps below 0.1 ensure good convergence. The discrete

energy evolution has a decrease tendency, which is foreseeable from the gradient-form governing equation. This approach is recommended when starting a PF simulation, in order to get the good range of values for which the discrete energy evolution has an optimum behavior.

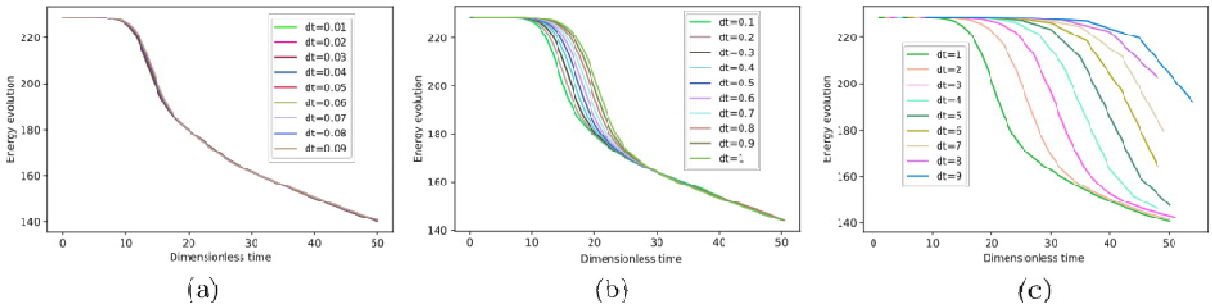

Figure 2: Energy evolution during spinodalTime vary from 0.01 to 0.09 in (a) from 0.1 to 1 in (b) and from 1 to 9 in (c).decomposition using a 2D grid. (a)

Once previous studies [7, 9, 17] have already proven the efficiency of adaptive time stepping compared to constant one, the choice of the time adaptivity approach for more complex models (KKS as illustrated here after) is here studied. Meanwhile, it should be reported that thisfirst trial is importantbecause it provides the appropriate range of the initial time step.

3.1.1 Method 1 of time stepping

Method 1 for adaptive time-stepping was applied on a 2D grid (N_x=N_y=128). The parameters $\triangle t_{min}$, $\triangle t_{max}$, α and initial time step (noted dt_{min}), from equation 10 are varied to observe their influence. Results are shown in Figure 3. The parametersα, $\triangle t_{min}$ and$\triangle t_{max}$ are varied in Figures 3a, 3b and 3c respectively. One can highlight different advantages of the use of this method. First, is the reasonable CPU time ($\sim$ 70s). Moreover, the range of parameters allowing convergence of the solution can be easily found and a tolerance in the choice of this triplet is here permitted. Indeed, increasing α up to 25, or $\triangle t_{max}$ (dimensionless) up to 5 or $\triangle t_{min}$ to 0.5 lead to approximately the same energy evolution and then the same microstructural changes. However, after a continuous decrease of the discrete energy, an oscillation zone, for some tested parameters, is observed close to the steady state (equilibrium). This numerical oscillation zone could be explained by the form of the equation 10, is based on the square of the discrete energy derivative. It may enhance small fluctuation when reaching the steady state. Comparing to a constant time-stepping methodology, Method 1 ensures an appı The infinite norm($\left|\left|X_n - X_{n-1}\right|\right|_\infty$), in Fig. 3d, explains more this trend because difference between actual concentration (X $_n$) and the previous one (X $_{n-1}$) is noticeable in early time then it gradually decreases. It should be noted that the peak observed at the end of the simulation would be a numerical issue and becomes obvious when allowing more time to simulation. Fig. 3f shows the evolution of the residual of the discrete energy; the green curve corresponds to the energy derivative, the left term in equation 10, while the red curve is associated to the right term and is the functional of potential gradient. It can be inferred that the energy derivative is dominant in early times while the potential gradient functional controls the residual trend in later times. To summarize, residual evolution traduces a good trend for the spinodal decomposition and the convergence of the solution. However, it should be noted that the decomposition is not finished as the residual and energy derivative curves do not yet reach a plateau. Hereafter, results of the complete simulations of both methods are illustrated for comparison purposes.

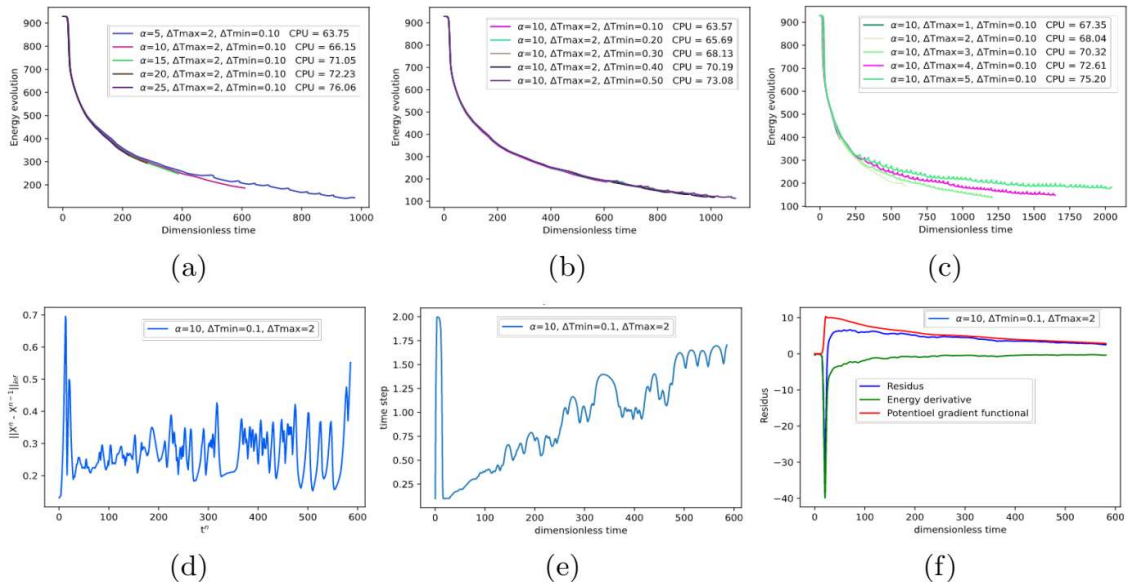

Figure 3: Influence of the variation of the different parameters of equation 10 on the energy evolution during simulation (using Method 1): (a) α (b) $\triangle t_{min}$ and (c) $\triangle t_{max}$. The evolution of infinite norm, time step and residual are respectively shown in (d), (e) and (f).

Some drawbacks should be highlighted about Method 1. Indeed, it takes in account only the left term of equation 10 (the energy derivative) while the right term is ignored. Once the variation of the gradient of chemical potential become more and more important and drives the evolution of energy residual, it becomes necessary to consider it to get accurate results. In addition, as shown in Fig. 3f, the infinite norm curve presents some strange oscillationsat simulation end, that cannot be due to physical parameters but only to numerical issues. Even for energy, it is noticed that oscillations are present in the energy curve after the dimensional time (t*=600), while time step oscillates between $\triangle t_{min}$and $\triangle t_{max}$. This drawback eventually affects the energy residual evolution by causing also an oscillatory behavior by the end of the simulation.

To apply the Method 2 of time stepping on equation 1, and for comparison purposes, the same parameters are used in the simulation. A first numerical experiment is conducted to identify the good range of *resmax* and *resmin* values. The values of energy equivalent values *resmin* and *resmax* are set to 1 and 30 respectively. This choice is indeed ensured by trial and error and is not a trivial task as already reported in [9]. These values are indeed very dependent on the physical inputs.

3.1.2 Method 2 of time stepping

The results of method 2 application are shown in Fig. 4. One has to mention the reasonable CPU time for the simulation using this methodology of time-stepping although it is an iterative algorithm. Moreover, the norm criterion ensures that energy residual should remain between *resmin* and *resmax*, else the actual iteration is redone. However, some issues should be reported about Method 2. At early times, when energy residual is less than resmin, the algorithm increases the time step at each iteration. On the one hand, when the time step is too high, that can influence the accuracy of the computed results. On the other hand, when the time step is too low, no improvement in the solution is observed and its gradual decrease results in non-physical solution and then divergence. This trend is well observed in simulations conducted using Method 2. Indeed, as shown inin Fig. 4c, by the beginning of the simulation, the time steps increases from (t^*=0.1) to 2 and remains constant. Consequently, the energy exhibits a slow

decrease rate, compared to results obtained by method 1, as illustrated in Fig. 4a .Moreover, the infinite norm (Fig.4b), which traduces the energy decay, cannot be decreased. Similarly, the energy residual (Fig. 4d) reaches a plateau and the solution cannot be improved by decreasing time step.If we try to decrease *resmax* to check the capability of this adaptive algorithm, the time step is gradually decreased which results in an exponential increase of the energy residual. As a result, simulation diverges.

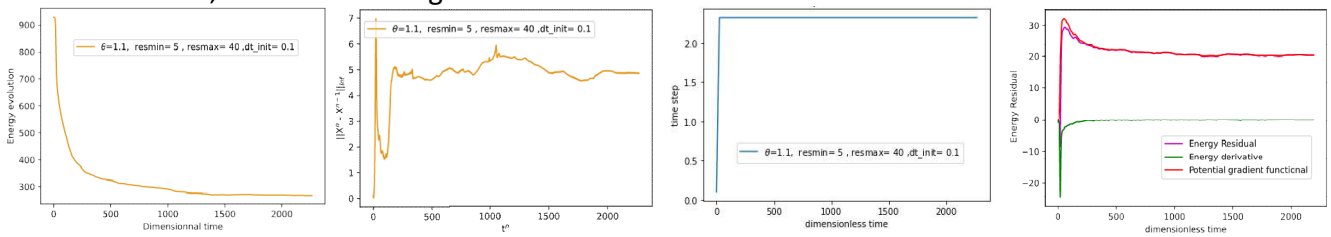

(a) (b) (c) (d)

Figure 4: Influence of the variation of the different parameters of equation 10 on the energy evolution during simulation (using Method 2): (a) energy e (b) infinite norm, (c) time step evolution and (d) energy residual.

3.1.3 Need for more accurate time stepping methodology

Advantages and inconvenient of methods 1 and 2 of adaptive time stepping could be summarized as follows. Method 1 ensures an accurate computation of the spinodal decomposition in a reasonable CPU time by adapting time step at each iteration in function of the variation of energy derivative. However, the residual of energy is not controlled. For method 2, the residual is forced to remain between 2 limits. Meanwhile, the continuous decrease of time step, when residual value is above *resmax,*can lead to divergence. To overcome these issues, we propose an alternative (called hereafter Method 3) which can be described as a combination of method 1 and method 2. The proposed algorithm is as follows.

- Step 1: compute X^{n+1} and obtain: $RE^{n+1} = \frac{\epsilon(\phi^{n+1})-\epsilon(\phi^n)}{\triangle t^n} + \int_V |\nabla \mu^{n+\frac{1}{2}}|^2 dV$
- Step 2: if $RE^{n+1} > resmax$:
  - Repeat this iteration: take $\triangle t^{n+1} = \triangle t^n/\theta$ and go to step 1
  - if the number of iteration exceeds 10, define the new time step as:

$$\triangle t = max(\triangle t_{min}, \frac{\triangle t_{max}}{\sqrt{1+\alpha\ G'(t)^2}})$$

Then, go to the next step.

- Step 3: if $RE^{n+1} < resmin$ take

$$\triangle t = max(\triangle t_{min}, \frac{\triangle t_{max}}{\sqrt{1+\alpha\ G'(t)^2}})$$

and go to the next step.

Here, no additional parameters are introduced compared to Method 2. Indeed, $\triangle t_{min}$ is the initial time step, while $\triangle t_{max}$=10*$\triangle t_{min}$. By this way, while (RE $\prec$*resmin*), the time step is adapted basing on the energy derivative criteria, which prevents it from gradual increase in some physical cases (e.g. the system needs to store enough energy at isothermal heating before starting phase transformation). Similarly, when (*RE*$\succ$*resmax*) and residual could not be decreased by 10 iterations, the algorithm expects a continuous decrease of time step values and acts to prevent that happen. Depending on the energy residual curve, a trial and error approach can be remade in order to better adjust *resmax* and *resmin* values. Results of energy evolution and residual are illustrated in Fig.5. One can remark the good behavior of infinite norm evolution as well as the energy residual. Comparing to Method 2, resmax is not increased; the algorithm

has the capability to decrease the value of residual at each step. Therefore, a continuous decrease of the system energy is ensured and simulation of microstructure evolution is guaranteed. It should be also noted that this methodology avoid strange numerical behavior observed with Method 1 (Fig. 3).

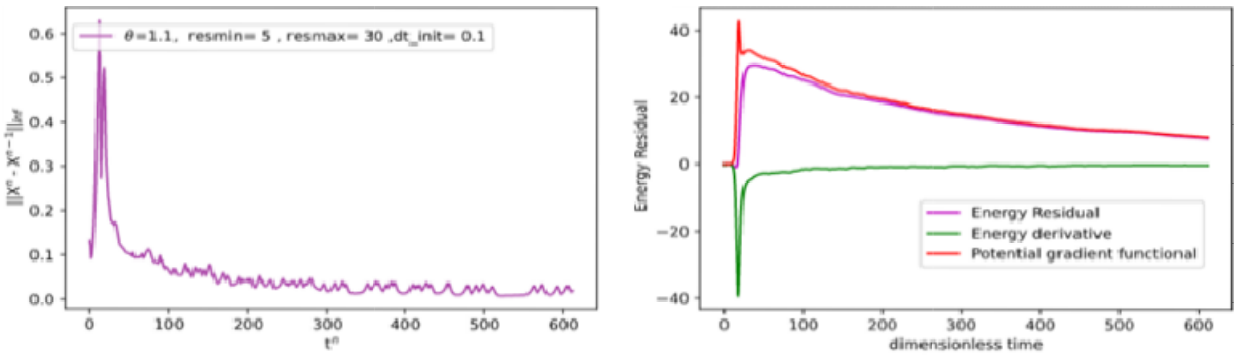

(a) (b)

Figure 5: Infinite norm (a) and energy residual (b) evolution (using Method 3).

In in Fig. 6a, a comparison is presented between the three methods. Using Method 3, the energy significantly decays with time and the decomposition is ensured. As it is an iterative method, CPU time is higher than with Method 1. Simulation time can be optimized using different numerical approaches in particular parallelization. For codes developed in Python environment (our case), optimization of computing time can be ensured through JIT (just in time) library [18]. Numba, the open source compiler in python environment, uses JIT compilation to translate its subsets as well as NumPy and Python to fast machine code. To apply it,"@jit" decorator can be implemented as a header of time-consuming functions to intensively compute then. It should be also noted that code implementation has a direct impact on computing speed. For that, spectral method has the advantage, comparing to FDschemes, to offer the possibility to minimize loops and directly apply functions on ND-arrays such as the application on the fast Fourier transform (fft) on the whole concentration matrix instead of looping on all grid points. By combining different optimization strategies, it is supposed to get accurate solutions in reasonable CPU time. This is one of goals of this ingoing work. The computing speed of fft schemes, compared to a classical FD one, can be demonstrated using 1D grids with different dimensions (from N_x=64 to 1024). Associated results are shown in Fig.6b.

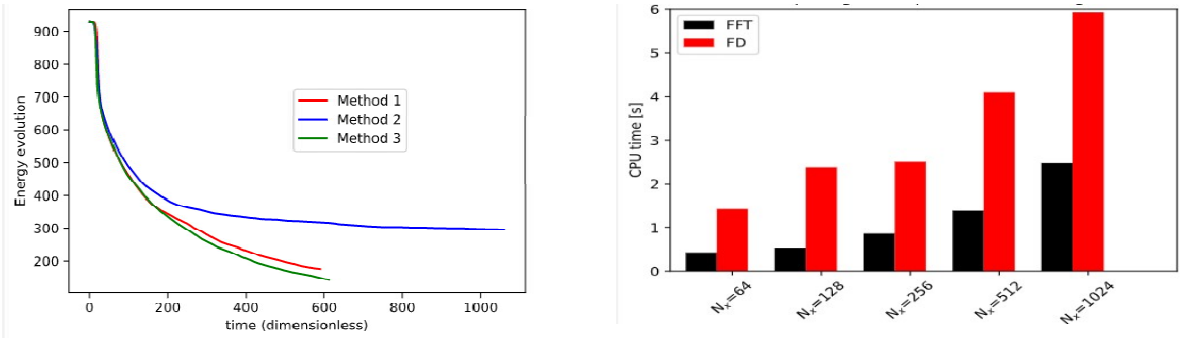

(a) (b)

Figure 6: (a) Energy evolution using Method 1, 2 and 3 of adapting time stepping (b) CPU time difference between spectral method and FD scheme.

3.1.4 Microstructure evolution

Microstructure evolution using Method 3 during spinodal decomposition is illustrated in Fig. 7. A 2D grid is here used using the optimum parameters of time stepping already obtained. For the 3D morphology, a grid (N_x=N_y=64) is used. The initial homogeneous morphology tends to separate into a binary alloy by aging time.We propose a comparison between spinodal decomposition using a constant time step on the one hand and adaptive time stepping on the other hand. The constant time step is chosen verysmall (t*=0.01) so the computed microstructure is used as reference. Results are shown in Fig. 7. Microstructure evolution using constant time stepping is illustrated in Fig.7a to e, while those of adaptive time stepping is shown in Fig.7f to j. Energy evolution using both schemes is shown in Fig.7 .k. Results of the adaptive time stepping method are close to the reference. Some points corresponding to differences in schemes are chosen in order to illustrate the maximum differences between computed grids.Obtaining the exact morphologies is not a trivial task when time schemes are different [19]. Current results are acceptable. An additional comparison is ensured in 3D as shown in Figs. 7 l to n. Similar decompositions are checked.

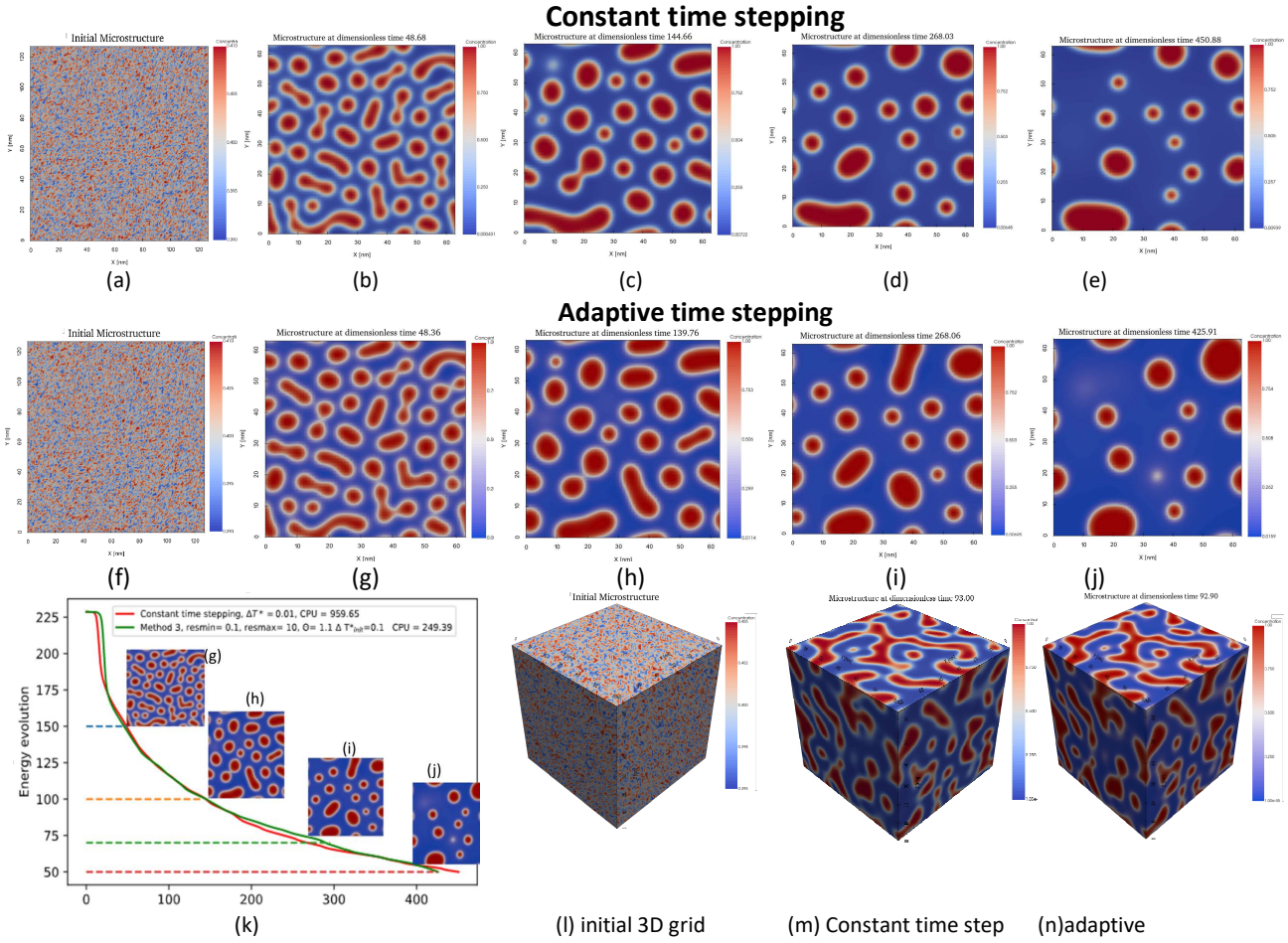

Figure 7: Spinodal decomposition using 2D grid (a to k) and 3D one (l to n).

3.2 Growth and coarsening of Si precipitates

3.2.1 Implementation of KKS model and results in 1D

Coarsening of Si precipitates in AlSi10Mg, approximated to a binary alloy, is studied using the KKS model, by resolving both equations 1 (CH) and 7 (AC). The proposed simulation targets, in 1D, 2 precipitates distributed along a 1D Grid (100Δx) for simplification purposes. It should be

noted that grid dimensions for this case of simulations are suggested to be higher (e.g. 2048 Δx in [20] to better control interface diffusion. At this stage, we target comparing computing speed and numerical behavior of the different simulation criterion: energy, residual, infinite norm etc.

The temperature is constant and set to 400K. The chemical energy in equation 8 is defined as:

$$f_{chem}(X,\eta,t) = (1-h(\eta,t).f^{\alpha}(X^{\alpha},\eta,t) + h(\eta,t).f^{\theta}(X^{\alpha},\eta,t) + w.g \quad (12)$$

Here h is a monotonous function, f^{α} and f^{θ} are the chemical free energy of α(α Al fcc) and θ(d-Si diamond) phases respectively, *g is a double well potential function and w* is the height of the double well potential.The most important parameters for the simulation are summarized in Table 1. Elastic strain energy due to precipitates misfit is not considered.

Table 1. Values of the most important parameters used in the 1D simulation of growth and coarsening of precipitates using KKS model.

Model parameter	value	Model parameter	value
Molar composition of the matrix AL and precipitates d-Si in Si $X^{Si}_{Al_{init}}$, $X^{Si}_{d-Si_{init}}$	0.03, 0.99	Interface mobility coefficient M_{η}	$2.42\ 10^{-22}$[$m^4s^{-1}J^{-1}$]
Al/Si Inter-diffusivity *D*	$2.52\ 10^{-16}$ [m^2s^{-1}]	*Kinetic coefficient for interface L*	$5.92\ 10^{-14}$ [$m^3s^{-1}J^{-1}$]

For the KKS model, adaptive time stepping is based on the computing of two residuals, associated to AC and CH equations respectively:

$$R^{n+1} = \frac{E(\eta^{n+1})-E(\eta^{n})}{dt^{n}} + \begin{cases} \frac{1}{\gamma}\int_V \left(\frac{\eta^{n}-\eta^{n+1}}{t^{n}}\right)^2 dV \\ \gamma \int_V |\nabla \mu^{n+1/2}|^2_{L_2} dV \end{cases} \quad (13)$$

Here γ donates the mobility. Results of the numerical experimental is shown in Fig. 8. The diffusion of the interface can be observed and is triggered by the interaction of chemical, gradient-effect and elastic energies. The interface position progressively changes duringthe isothermal aging. In the simulations, the two precipitates whose initial width is (w= 6.△x), a trend to diffuse and coalescence is expected for long time of heating. Results are shown in Fig. 8. Si concentration (X_{Si}) and order parameter (η) are computed for 15000 steps using adaptive scheme (Figs. 8 c and d). We found that the same evolution is reproduced by 150000 steps and approximatively 10 times longer using a constant time step (Figs. 8 a and b). The proposed method ensure indeed accurate computing and avoid losing too much computational time.

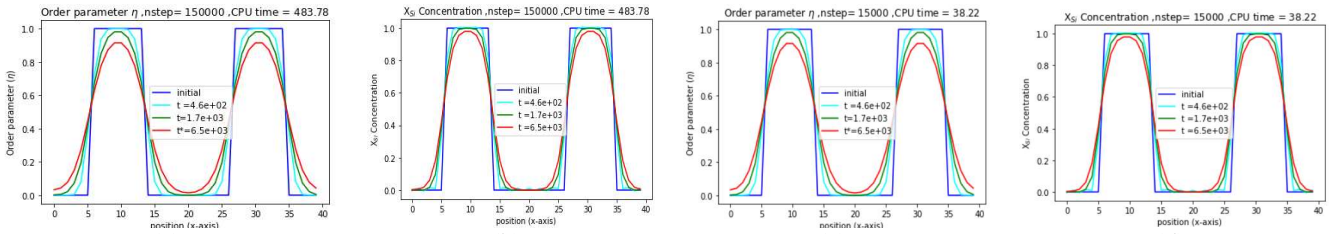

(a) (b) (c) (d)

Figure 8: Evolution of order parameter (η) and Si concentration with the coarsening of precipitates.

3.2.2 Toward the prediction of the thermo-physical properties and tensile strength of AlSi10Mg

The elastic energy in the system due to the volume misfit between the precipitates and the matrix will be considered. Such results are to be post-processed to provide thermo-physical

properties (thermal conductivity and specific heat capacity) as well as mechanical properties (elasticity). The values based on numerical predictions are compared to the ones deduced from experimental measurement in particular for differential scanning calorimetry (DSC), dilatometry, laser flash diffusivimetry (LFA) and micro or nano-indentation experiments. Once validated, the methodology is expected to offer a quick and efficient properties prediction for different thermal post treatments.

4 Conclusions

In this work, the spinodal decomposition and precipitates growth in a binary alloy (the target is AlSi10Mg) were investigated. We have shown that adaptive time stepping is very important to keep energy residual in an appropriate range and to ensure the decay of the system energy during evolution. Different approaches of time stepping were investigated: constant time stepping, a non-iterative method and an iterative one. An optimization of the iterative method was ensured for the spinodal decomposition. Then, 1D, 2D and 3D simulations were conducted in order to validate the approach. Such a method is of great importance to be applied when the PF field model should take into account the different forms of energy, which is the case of the KKS model. A first implementation, in 1D, of the KKS model was shown to prove its capability of studying the growth and coarsening as well as concentration evolution of Si in precipitatesand inside the aluminum matrix. We used different criterion to evaluate performances of simulations of microstructural changes: energy, residual, potential gradient, infinite norm and time step evolutions.

The robust implemented model is a mandatory step toward prediction of microstructural changes, elastic and thermo-physical properties when correlating phase-field results with Calphad data.

5 Data availability

The python code, needed to produce the results obtained in section 3.1 can be shared, while results of section 3.2cannot at this time. The related work is ingoing.

References

[1] J. Delahaye, J. TchoufangTchuindjang, J. Lecomte-Beckers, O. Rigo, A.M. Habraken, A. Mertens, Influence of Si precipitates on fracture mechanisms of AlSi10Mg parts processed by Selective Laser Melting, ActaMaterialia, Volume 175, 2019, Pages 160-170,https://doi.org/10.1016/j.actamat.2019.06.013

[2] Félix A. España, Vamsi Krishna Balla& Amit Bandyopadhyay (2011) Laser processing of bulk Al–12Si alloy: influence of microstructure on thermal properties, Philosophical Magazine, 91:4, 574-588, https://doi.org/10.1080/14786435.2010.526650

[3] FeiyuXiong, Chenyang Huang, Orion L. Kafka, YanpingLian, Wentao Yan, Mingji Chen, Daining Fang, Grain growth prediction in selective electron beam melting of Ti-6Al-4V with a cellular automaton method, Materials & Design, Volume 199, 2021,109410, https://doi.org/10.1016/j.matdes.2020.109410.

[4] Provatas, N., Dantzig, J.A., Athreya, B. et al. Using the phase-field crystal method in the multi-scale modeling of microstructure evolution. JOM 59, 83–90 (2007). https://doi.org/10.1007/s11837-007-0095-3

[5] Kim SG, Kim WT, Suzuki T. Phase-field model for binary alloys. Phys Rev E Stat Phys Plasmas Fluids RelatInterdiscip Topics. 1999 Dec;60(6 Pt B):7186-97. https://doi.org/10.1103/PhysRevE.60.7186

[6] Larry K. Aagesen, Daniel Schwen, Karim Ahmed, Michael R. Tonks, Quantifying elastic energy effects on interfacial energy in the Kim-Kim-Suzuki phase-field model with different interpolation schemes, Computational Materials Science, Volume 140, 2017, Pages 10-21, https://doi.org/10.1016/j.commatsci.2017.08.005.

[7] Zhengru Zhang, Yuan Ma, ZhonghuaQiao, An adaptive time-stepping strategy for solving the phase field crystal model, Journal of Computational Physics, Volume 249,2013,Pages 204-215,ISSN 0021-9991,https://doi.org/10.1016/j.jcp.2013.04.031.

[8] YYibao Li, Yongho Choi, Junseok Kim, Computationally efficient adaptive time step method for the Cahn–Hilliard equation, Computers & Mathematics with Applications, Volume 73, Issue 8, 2017, Pages 1855-1864, ISSN 0898-1221,https://doi.org/10.1016/j.camwa.2017.02.021.

[9] Francisco Guillén-González, Giordano Tierra, Second order schemes and time-step adaptivity for Allen–Cahn and Cahn–Hilliard models, Computers & Mathematics with Applications, Volume 68, Issue 8, 2014, Pages 821-846, ISSN 0898-1221, https://doi.org/10.1016/j.camwa.2014.07.014.

[10] R. Backofen, A. Rätz& A. Voigt (2007) Nucleation and growth by a phase field crystal (PFC) model, Philosophical Magazine Letters, 87:11, 813-820, https://doi.org/10.1080/09500830701481737

[11] Mowei Cheng, James A. Warren, An efficient algorithm for solving the phase field crystal model, Journal of Computational Physics, Volume 227, Issue 12, 2008, Pages 6241-6248, https://doi.org/10.1016/j.jcp.2008.03.012.

[12] Yoon, S.; Jeong, D.; Lee, C.; Kim, H.; Kim, S.; Lee, H.G.; Kim, J. Fourier-Spectral Method for the Phase-Field Equations. Mathematics 2020, 8, 1385. https://doi.org/10.3390/math8081385

[13] L.Q. Chen, Jie Shen, Applications of semi-implicit Fourier-spectral method to phase field equations, Computer Physics Communications, Volume 108, Issues 2–3, 1998, Pages 147-158, ISSN 0010-4655, https://doi.org/10.1016/S0010-4655(97)00115-X.

[14] Kuhl, E., Schmid, D.W. Computational Modeling of Mineral Unmixing and Growth. ComputMech 39, 439–451 (2007). https://doi.org/10.1007/s00466-006-0041-1

[15] Roy H. Stogner, Graham F. Carey, and Bruce T. Murray. Approximation of Cahn-Hilliard di use interface models using parallel adaptive mesh refinement and coarsening with c1 elements. International Journal for Numerical Methods in Engineering, 76:636-661, 2008.https://doi.org/10.1002/nme.2337

[16] Phase- Field simulations of coarsening kinetics of Si precipitates in alsi10mg processed by selective laser melting. Orbit Uliège, Scientific congresses and symposiums : Unpublished conference, 2020.https://doi.org/10.1002/nme.2337

[17] Héctor Gómez, Victor M. Calo, Yuri Bazilevs, Thomas J.R. Hughes, Isogeometric analysis of the Cahn–Hilliard phase-field model, Computer Methods in Applied Mechanics and Engineering, Volume 197, Issues 49–50, 2008, Pages 4333-4352, https://doi.org/10.1016/j.cma.2008.05.003.

[18] Jan Gmys, Tiago Carneiro, NouredineMelab, El-GhazaliTalbi, Daniel Tuyttens, A comparative study of high-productivity high-performance programming languages for parallel metaheuristics, Swarm and Evolutionary Computation, Volume 57, 2020, 100720, https://doi.org/10.1016/j.swevo.2020.100720.

[19] Zhang, Z., &Qiao, Z. (2012). An Adaptive Time-Stepping Strategy for the Cahn-Hilliard Equation. *Communications in Computational Physics, 11*(4), 1261-1278. https://doi.org/10.4208/cicp.300810.140411s

[20] S.Y. Hu, J. Murray, H. Weiland, Z.K. Liu, L.Q. Chen, Thermodynamic description and growth kinetics of stoichiometric precipitates in the phase-field approach, Calphad, Volume 31, Issue 2, 2007, Pages 303-312, https://doi.org/10.1016/j.calphad.2006.08.005.